

Chapter 4

Influence of carbon sources on the biofilm community in denitrifying conditions

4.1. Introduction

It was seen in the previous chapter that nutrients modulate the biofilm architecture of a single population. Also nutrients select organisms in communities and the selected community in that particular environment can also change the architecture of the biofilm. Biofilm structure can significantly influence the activity as was seen in the previous chapter.

An exogenous carbon source has to be provided as an electron donor for efficient nitrate removal by denitrification (Mateju et al. 1992; Park & Yoo 2009). The widely used carbon sources in denitrifying reactors are methanol, acetate, ethanol and glucose (Mateju et al. 1992; Her & Huang 1995; Constantin & Fick 1997; Dincer & Kargi 2000; Ginige et al. 2005). Though numerous studies have reported on the usage of different carbon sources for nitrate removal, they have dealt mostly on the kinetics of denitrification and very few have reported on the communities involved.

Hence the aim of this study was to holistically determine the factors affected by the different exogenous carbon sources on the denitrifying biofilm. Denitrifying activity, abundance of *nosZ* gene, biofilm structure including succession in the community were analysed as influenced by acetate, glucose, methanol and ethanol.

4.2. Materials and Methods

4.2.1. Reactor description

A 1 L laboratory-scale reactor made up of silica glass was used for the biofilm studies with polystyrene slides suspended in the reactor for the biofilm development (Fig. 4.1). The influent synthetic wastewater for 1000 ml of reverse osmosis (RO) water consisted of Na_2HPO_4 0.64 mg, KH_2PO_4 0.15 mg, NaCl 0.25 mg, NH_4Cl 0.48 mg, MgSO_4 24 mg, CaCl_2 1.1 mg, KNO_3 1.0 g and the carbon sources used were acetate, glucose, methanol and ethanol with a carbon to nitrate ratio of 2.5 and the medium pH was maintained at 7.0. The reactor was operated continuously with a flow rate of 0.12 L Hour^{-1} . The biofilm was allowed to establish with each carbon source for 30 days in the order acetate, glucose, methanol and ethanol and the effluent was sampled to estimate nitrate, nitrite

and ammonium. Two polystyrene slides were removed from the reactor after each batch of 30 days for microscopy and extraction of DNA which was replaced by two sterile slides in the reactor. During each transition of carbon source, 2.5% of sludge was used to seed the reactor from a fertilizer company aeration tank. The synthetic wastewater in the reactor was stirred slowly by a magnetic stirrer at the bottom. The temperature was maintained at 30°C.



Fig. 4.1. The 1L laboratory-scale biofilm reactor in which polystyrene slides were immersed for the biofilm development on it. The synthetic wastewater in the reactor was mixed by a magnetic stirrer below.

4.2.2. DNA extraction from the biofilm

The polystyrene slides were rinsed in sterile saline to remove any unbound planktonic cells and biofilm cells were scraped off the polystyrene slides with a rubber policeman and suspended in 6 ml of sterile saline. The cells were centrifuged at 4000 g for 10 minutes and washed twice with sterile saline. 500 μ l of lysis buffer (100 mM Tris HCl

pH 8.0, 100 mM Sodium EDTA pH 8, 100 mM Sodium Phosphate pH 8, 1.5 M Sodium Chloride, 1.5% Cetyl Triammoniumbromide) was then added along with 16 µl of 20% sodium dodecyl sulphate and 5 µl of proteinase K (10mg/ml). The mixtures were then vortexed vigorously and incubated at 37°C for 1 hour. The DNA was separated using the phenol, chloroform and isoamyl alcohol mixture (25:24:1). The aqueous layer was extracted and precipitated with 0.6 volumes of isopropanol, centrifuged at maximum speed for 10 minutes, the supernatant was discarded and pellet washed twice with 70% ethyl alcohol. The microfuge tubes were centrifuged in a Speed Vac (Thermo Scientific) for 10 minutes for complete evaporation of the alcohol. The pellet was then suspended in 25 µl of Tris EDTA pH 8.0 and treated with RNase. The extracted DNA was run on 8% agarose gel to confirm its presence.

4.2.3. Quantitative Real time PCR

The gene *nosZ*, which codes for the nitrous oxide reductase in denitrifying bacteria and 16S rRNA gene for all bacteria were, quantified with SYBR green master mix (Applied Biosystems) with a 20 µl reaction system in StepOne real time PCR (Applied Biosystem) by the standard curve method. Standard curves were constructed with the plasmid containing insert of respective genes. PCR conditions and primers (*nosZF2* and *nosZR2*) used for *nosZ* were according to Henry et al. (2006) with a touchdown PCR. Primers used for 16S rRNA gene were 340f (5'-CTACGGGAGGCAGCAGTGGG-3') and 536r (5'-GTATTACCGCGGCTGCTG-3'). Conditions of PCR for 16S were, an initial denaturation temperature of 95°C for 10 mins, 40 cycles of PCR at 95°C for 15s, 30s at 62°C, and 72°C for 30s. The acquisition temperature for both the genes was set at 80°C for 15 seconds and No Template Controls (NTC) was run for each reaction in triplicates.

4.2.4. PCR - Denaturing Gradient Gel Electrophoresis (DGGE)

PCR - DGGE of the community was performed on the partial 16S rRNA gene. The primers used for DGGE was the same as mentioned above for the qReal-Time PCR except that the reverse primer was tagged with a 33 bp GC clamp (5'-GGC GGC GCG CCG CCC GCC CCG CCC CCG TCG CCC-3') at its 5' end. The DGGE was performed using the D-Code Universal Detection Mutation System (Bio-Rad). 8% polyacrylamide gels

having gradients of 40-70% denaturant were used to run the gel. The 100% denaturing solution strength was defined as 7 M urea and 40% formamide. The gel was run using TAE buffer for 16 hours at 60°C with 60 V and visualized by silver staining. The cluster and densitometric analysis of DGGE bands were performed using the GelCompar II software. The percent change in the communities was calculated according to the moving window analysis performed by Wittebolle et al. (2005). The selected bands were eluted and a re-PCR was performed for sequencing the amplicons. The sequencing was performed in the ABI 3730xl DNA Analyzer at services provided by XcelrisLabs. The Pubmed accession numbers of the sequences are JF737972 to JF737974, JF737976 and JF737978 to JF737984

4.2.5. Fluorescence *in Situ* Hybridization (FISH)

A multiplex FISH was performed with the oligonucleotide probes PSE227 (Watt et al. 2006) for *Pseudomonas* sp. linked to CY5, probe ALC-476 (Wellinghausen et al. 2006) linked to TAMRA and PAR651 probe (Neef et al. 1996) tagged with 6-FAM. The oligonucleotide probes were purchased from Eurofins MWG Operon and the FISH was performed according to established procedures (Daims et al. 2005), where the biofilm formed on the polystyrene slides were fixed with 4% paraformaldehyde for 3 hours at 4°C followed by permeabilization with three successive treatments of 50%, 80% and 96% ethanol for 3 minutes each. A 10 µl of hybridization buffer of 40% stringency containing the probes PAR651 and ALC- 476 was applied to the slides. The slides were incubated in a hybridization oven for 1.5 hours at 46°C. Subsequent to the hybridization step, the slides were washed by dipping them into pre-heated wash buffer at 48°C for 15 minutes. The procedure was repeated for lower stringency probe PSE227.

4.2.6. Image analysis

Image acquisition was done in Zeiss (LSM 510 Meta) confocal laser scanning microscope (CSLM). More than ten fields from each slide were randomly chosen to acquire images with constant microscopic settings. Raw images were processed by IMARIS and Adobe Photoshop softwares. Thresholding was manually done with constant values for all the image series and quantification of biofilm parameters were done by COMSTAT program written as a script in MATLAB 5.1 (Heydorn et al. 2000).

Densities for the FISH images in the different channels were measured by ImageJ, a NIH freeware (<http://rsb.info.nih.gov/ij/index.html>).

4.3. Results and Discussion

4.3.1. Carbon sources influence nitrate reducing activity of the biofilm

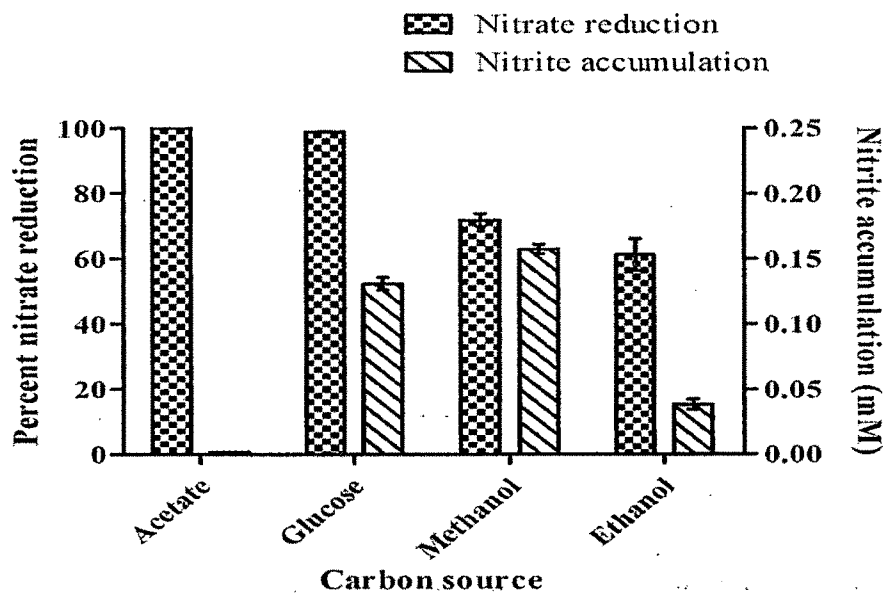
The activity by the biofilm community formed in presence of different carbon sources was analysed by estimating the nitrate, nitrite and ammonium concentrations in the influent and effluent after 30 days of biofilm establishment in a carbon source. A constant flow rate of 0.12 L hour^{-1} was maintained which corresponds to a retention time of 8.3 hours. Acetate and glucose biofilms reduced nearly 100% nitrate, while 72 and 61% nitrate was reduced by the methanol and ethanol biofilm respectively (Fig. 4.2a). Though glucose biofilm reduced nitrate efficiently, substantial nitrite accumulation was observed. However, nitrite build-up was highest in methanol biofilm with 0.157 mM and ethanol biofilm accumulated 0.038 mM nitrite. Methanol is the most widely used carbon source for denitrification in reactors, although a typical lag in the adaptation of the community has been observed before efficient denitrification (Hallin et al. 1996). However, higher denitrification rates have been obtained with acetate as a carbon source in other studies too (Lee & Welander 1996; Elefsiniotis et al. 2007).

The ammonium concentration in glucose biofilm increased by 213% from the influent while ammonium in ethanol biofilm decreased by 86%. No substantial increase or decrease was observed with methanol, whereas a 10% decrease was observed when acetate was the sole carbon source (Fig. 4.2b). Nitrate has different fates in the anoxic environment where it can be reduced to dinitrogen by the denitrification pathway, or a dissimilatory nitrate reduction to ammonium (DNRA) by nitrate ammonifiers (Strohm et al. 2007). The data suggests that the glucose biofilm is possibly dominated by the nitrate ammonifying bacteria. However, nitrate limiting conditions is shown to be the reason for the selection of nitrate ammonifiers (Tiedje et al. 1982; Strohm et al. 2007) but, the data (Fig. 4.2) suggests that the kind of carbon source can also increase them. Build-up of nitrite and ammonium in the medium and high nitrate reduction with glucose as the substrate was also observed by Akunna et al. (1993).

4.3.2. Abundance of denitrifying bacteria in the biofilm influenced by different carbon sources

The abundance of denitrifying bacteria was monitored in the biofilm by investigating the density of *nosZ* gene which codes for the nitrous oxide reductase, the last step of denitrification. Denitrifying bacteria have two different kinds of nitrite reductases NirK and NirS with each containing copper and cytochrome cd_1 respectively as their cofactors (Zumft 1997). Either of the reductases is present in a species, but never the both. Hence to overcome this redundancy, we targeted *nosZ* gene to investigate the abundance of denitrifiers, while 16S rRNA gene was targeted for enumerating the bacterial abundance in the biofilm. Standard curve was constructed by a series of ten dilutions with the respective plasmid inserts. PCR efficiency was more than 96% and standard curve with R^2 value of 0.99 was achieved. Melt curve for both the genes is shown in Fig. 4.3, where single peaks were found beyond 80°C. The acquisition temperature was set at 80°C. Abundance of both *nosZ* and 16S rRNA gene was significantly high in the glucose biofilm with *nosZ* gene copy number of $4.15 \times 10^9 \text{ cm}^{-2}$ and 16S gene copy number of $1.66 \times 10^{13} \text{ cm}^{-2}$ (Fig. 2a). *nosZ* gene copy number in the biofilm established in presence of other carbon sources showed a range of 10^8 cm^{-2} and 16S rRNA gene was 10^{12} (Fig. 4.4a). However, the *nosZ* percentage was higher in the ethanol biofilm with 0.29% and lowest in methanol biofilm with 0.004% (Table 4.1). The nitrate reduction was in contrast lowest in ethanol biofilm (Fig. 3.2a), but the nearly 86% decrease in ammonium concentration (Fig. 4.2b) along with nitrate suggests that the ethanol biofilm consists of denitrifier population in high numbers. Gomez et al. (2003) also observed increase in denitrifier population with increase in ethanol concentration.

(a)



(b)

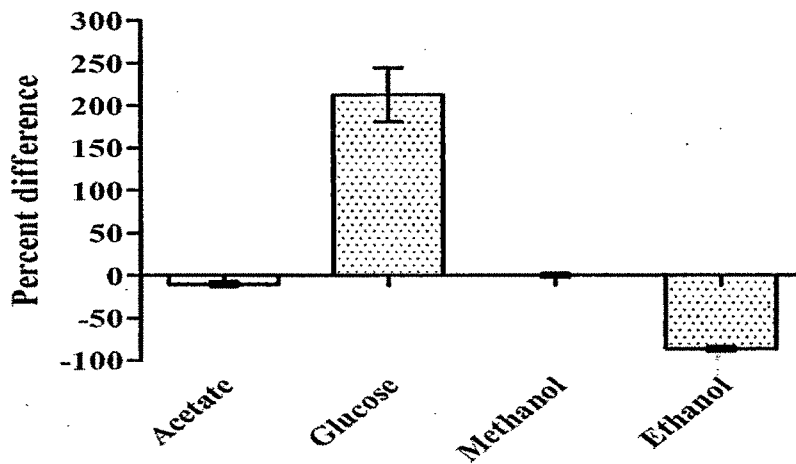


Fig. 4.2 . Activity of the biofilm in presence of different carbon sources (a) Denitrification activity and (b) Percent ammonium difference in the effluent of the reactor from the influent

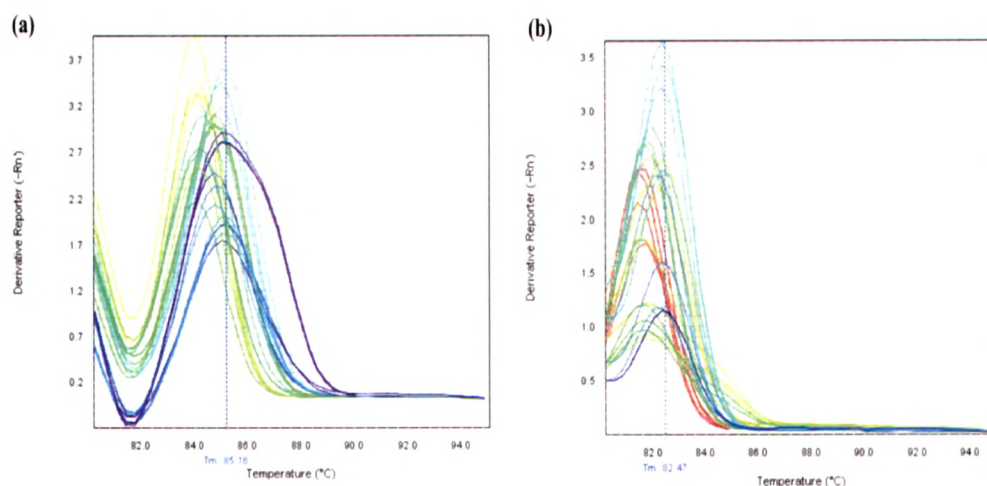
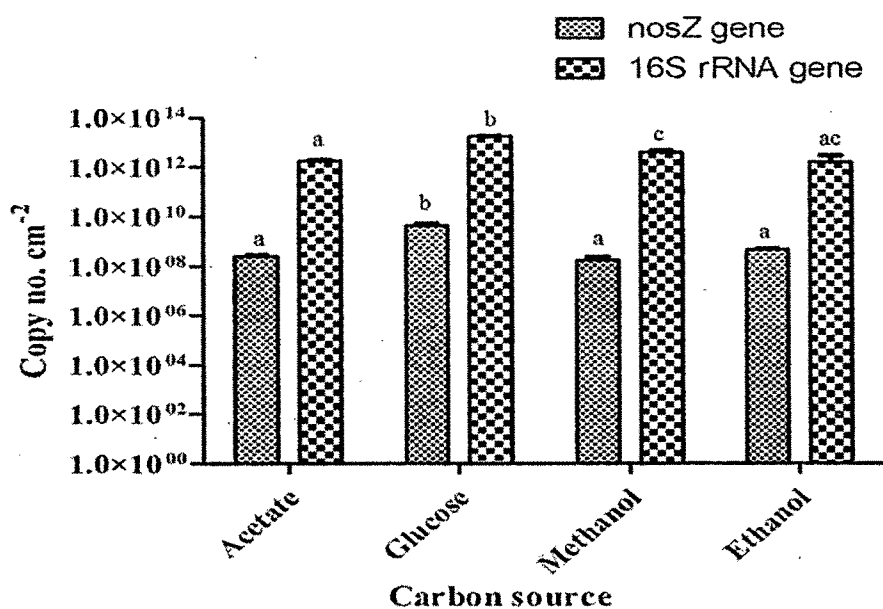


Fig. 4.3. Melt curve of the (a) *nosZ* gene and (b) 16S rRNA gene

The abundance of *nosZ* and 16S rRNA gene was also checked in the effluent to get an idea of the biofilm dispersal, where glucose biofilm showed a significantly higher copy number of *nosZ* gene ml^{-1} with 4.46×10^{10} , while biofilm formed with other carbon sources were in the range of 2.85×10^8 to 1.56×10^9 (Fig. 4.4b). The 16S rRNA gene detected in the effluent was in the range of 1.2×10^{13} to 7.25×10^{13} copy number ml^{-1} with acetate being the highest (Fig. 4.4b). However, the effluent to biofilm ratio of the *nosZ* gene percentage in glucose was very high with 2.9 (Table 4.1), suggesting a high dispersal of denitrifiers when glucose is used as carbon source. This is also consistent with the activity data (Fig. 4.2), which suggests the nitrate ammonifiers to be dominant in glucose biofilm. Acetate and ethanol biofilm showed comparable values for the effluent to biofilm ratio with low dispersal of denitrifiers (Table 4.1).

(a)



(b)

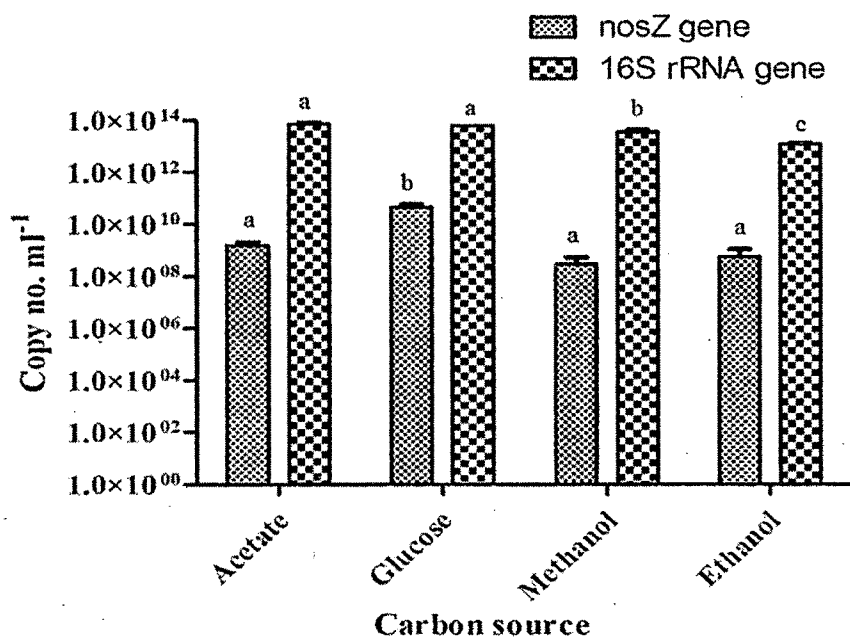


Fig. 4.4. Abundance of *nosZ* and 16S rRNA gene in the (a) Biofilm (b) Reactor effluent. Same letter above the bars indicate no significant difference. One way ANOVA with Tukey's test was used to determine significant differences ($p < 0.05$).

Table 4.1. Percentage of *nosZ* gene as analyzed from fig. 4.4 data

| Carbon source | Biofilm | Effluent | Effluent to Biofilm ratio |
|---------------|---------|----------|---------------------------|
| acetate | 0.014 | 0.002 | 0.142 |
| glucose | 0.024 | 0.070 | 2.916 |
| methanol | 0.004 | 0.0008 | 0.200 |
| ethanol | 0.029 | 0.004 | 0.138 |

4.3.3. The emergent biofilm architecture in different carbon sources

It was seen in the previous chapter that the nutrients determine the biofilm architecture which in turn modulates the function. The structural parameters of the biofilm formed under different carbon sources were examined and it was observed that the acetate and ethanol biofilms were mosaic-structured with the characteristic voids, whereas confluent biofilms were formed with glucose and methanol (Fig. 4.5). Labbe et al. (2007) also observed methanol-fed marine biofilm devoid of characteristic channels or voids. Biovolume significantly decreased in the following order acetate > glucose > methanol > ethanol (Fig. 4). Acetate also showed high ($p < 0.05$) thickness and diffusion distance (Fig. 4.6). Acetate biofilm showed a maximum thickness of 92 μm whereas methanol biofilm was lowest in maximum thickness with 49.5 μm . Average thickness of acetate biofilm was 73.7 μm , glucose with 41.9 μm and methanol and ethanol biofilms with 36.9 μm . Diffusion distance was significantly higher in acetate and glucose biofilms than the alcohols. Ethanol biofilm showed a significantly higher roughness coefficient (Fig. 4.6).

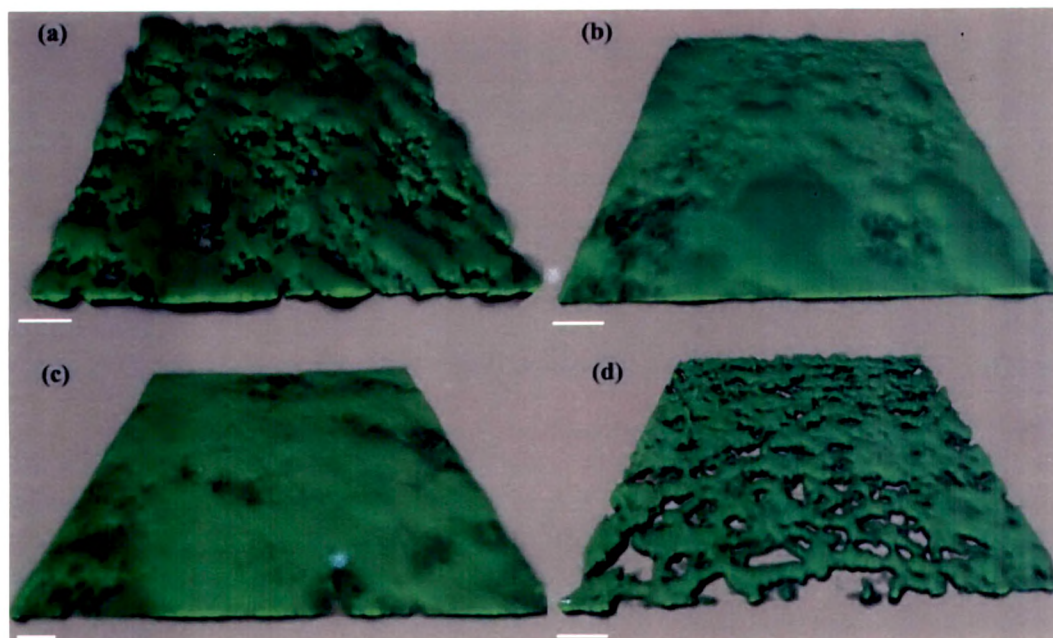


Fig. 4.5. The 3-D projection of representative biofilm CLSM images grown in different carbon sources. (a) Acetate (b) Glucose (c) Methanol (d) Ethanol. Scale bar = 100 μm

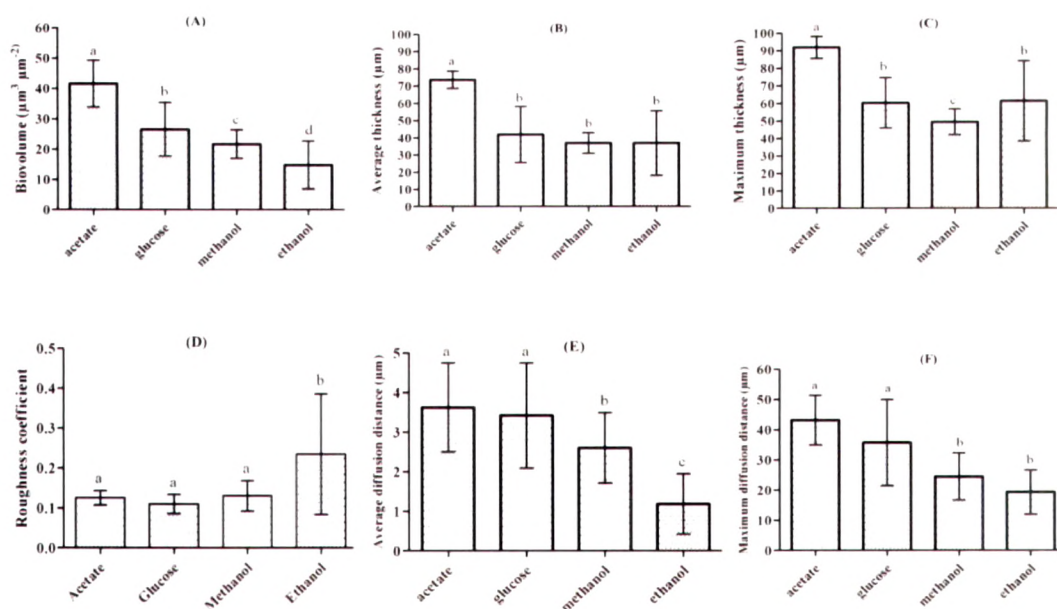


Fig. 4.6. Quantification results of the CLSM acquired biofilm images. (A) Biovolume (B) Average thickness (C) Maximum thickness (D) Roughness coefficient (E) Average diffusion distance (F) Maximum diffusion distance. . Same symbols above the bars indicate no significant difference. One way ANOVA with Tukey's test was used to determine significant differences ($p < 0.05$).

The thickness of the biofilm possibly decreases the diffusion of oxygen because the available oxygen is utilized by the organisms in the bulk phase and surfaces of the biofilm clusters. deBeer et al. (1994) showed decreased oxygen concentrations inside the cell clusters than the bulk fluid phase. Quantifying the denitrifying bacteria in the biofilm does not mean that their activity is also present (Philippot & Hallin 2005] because the nitrate reduction is regulated by oxygen sensitive FNR-like regulons which gets activated only in conditions where the partial pressure of the oxygen decreases (Zumft 1997). The high thickness with increased diffusion distances and high biovolume could also be the possible reason for high nitrate reduction in acetate and glucose biofilms. Similar results of increased denitrification activity in calcium and magnesium induced biofilm of *Paracoccus* sp. W1b with high thickness were observed in the previous chapter.

4.3.4. Biofilm community structure in different carbon sources

The community structure of the biofilm established under different carbon sources were analysed by the DGGE fingerprinting method. Each band was assumed as an operational taxonomic unit (OTU). Though there are limitations for this assumption in any DNA fingerprinting method (Bent et al. 2007), this was used for relative comparison and the analysis of the dominant phylotypes (Fig. 4.7). According to the moving window analysis (Fig. 4.8), a 27% change in community occurred when the carbon source was changed from acetate to glucose, but 71.5% community change was observed from glucose to methanol transition. Methanol to ethanol also had a 64% change of the biofilm community. Though a high rate of change in community was observed during the transition of carbon sources, glucose to methanol, a high diversity (Table 4.2) was found in both of these as compared to the acetate and ethanol biofilms. Acetate biofilm had the lowest diversity (Table 4.2). The evenness was above 0.8 with all the carbon sources while methanol showed highest evenness of 0.953 (Table 4.2).

Eleven prominent bands designated with the letters A to K (Fig. 4.7a) were eluted and sequenced, and the closely matched organism of these sequences is shown in Table 4.3. The intensity profile of the bands (Fig. 4.7c) indicates the abundance of the organisms, where proportional intensities of glucose and methanol biofilm are comparatively lower than those in ethanol and acetate biofilms. The glucose and methanol biofilm consisted of bands not with more than 20% density, whereas the bands in acetate biofilm had more

than 20% density. The bands E and H consisted of 23 and 20% with their sequences showing similarity to different *Pseudomonas* species in acetate biofilm while the band F in ethanol biofilm was 20% having similarity to another *Pseudomonas* sp. (Table 4.3). Abundance of above 10% density was found for E, G, H, J, and K in the glucose biofilm with sequence similarity of the E, G and H corresponding with diverse *Pseudomonas* sp. and *Alcaligenes* sp. respectively, while J and K sequences were similar to different *Enterobacter* sp. (Table 4.3).

The low evenness in the ethanol and acetate biofilms (Table 4.2) can be attributed to the dominant *Pseudomonas* sp. Ethanol is utilized by the organisms by converting it to acetate by an acetaldehyde intermediate (Constantin & Fick 1997), thus acetate serving as the electron donor for both ethanol and acetate biofilms, which could be the possible reason for the high density of different *Pseudomonas* species. It was seen that the band J corresponding to the *Enterobacter* sp. and band K corresponding to an uncultured bacterium clone belonging to the Enterobacteriaceae family consists of 16 and 12% of the glucose biofilm (Table 4.3). Enterobacteriaceae group members are implicated in the nitrate ammonification process (Rutting et al. 2011). The increase of the Enterobacteriaceae members is the possible reason for the ammonium build-up (Fig. 4.2b) in the glucose biofilm. Methanol biofilm is dominated by band A (Fig. 4.7c) corresponding to *Methylobacillus* sp. (Table 4.3) which are known to grow on methanol (Urakami & Komagata 1986; Kim et al. 1991). The bands G and H corresponding to *Alcaligenes faecalis* and *Pseudomonas* sp. respectively (Table 4.3) are present ubiquitously in all the biofilm with the carbon sources used in high density.

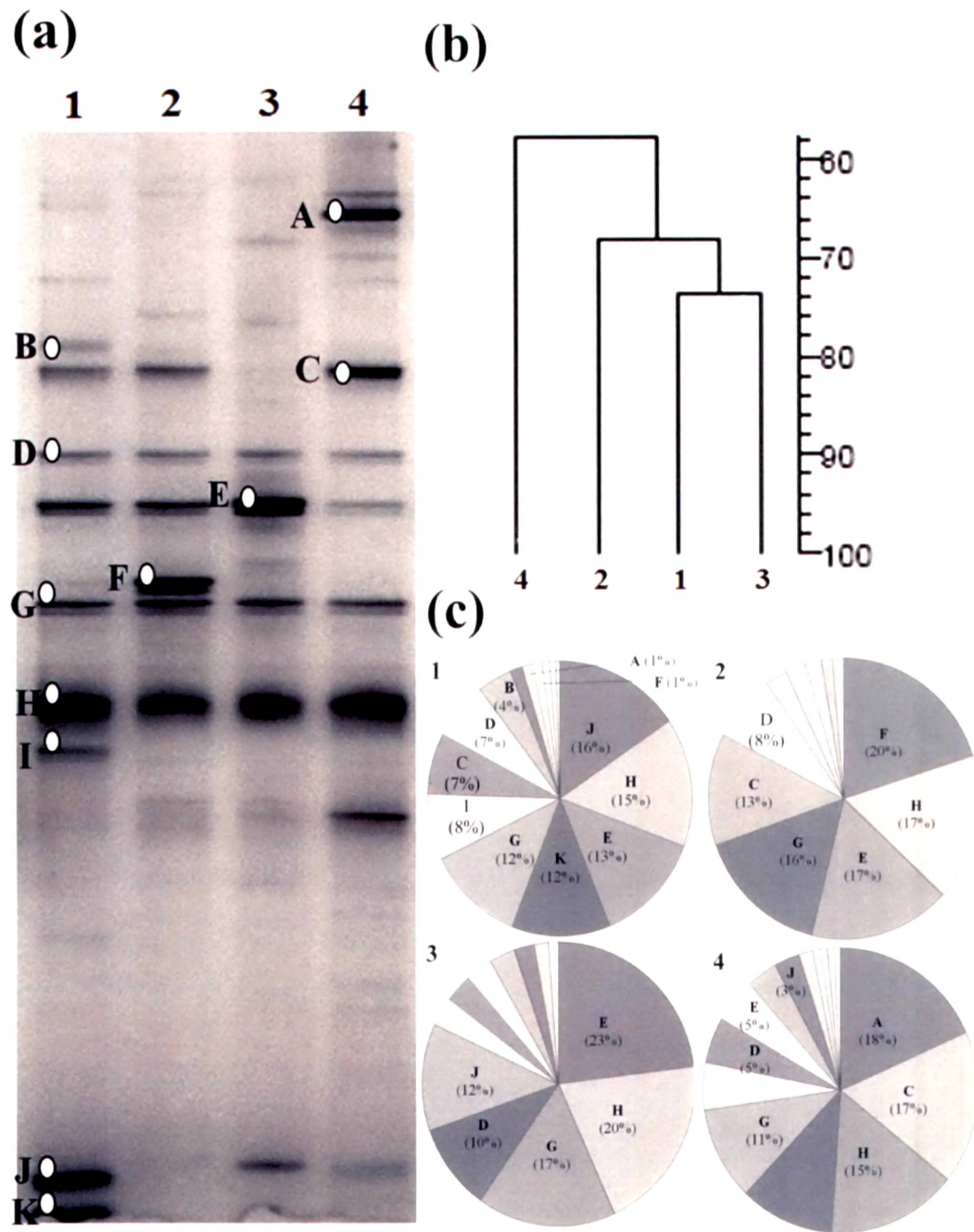


Fig. 4.7. (a) DGGE image of 16S rRNA gene amplicon from the biofilm formed in different carbon sources (b) Cluster analysis based on Pearson coefficient constructed by UPGMA method. (c) Pie chart displaying the intensity profile. Letters A to K are the sequenced bands. 1. Glucose, 2. Ethanol, 3. Acetate, 4. Methanol. Parenthesis contains the percentage intensity.

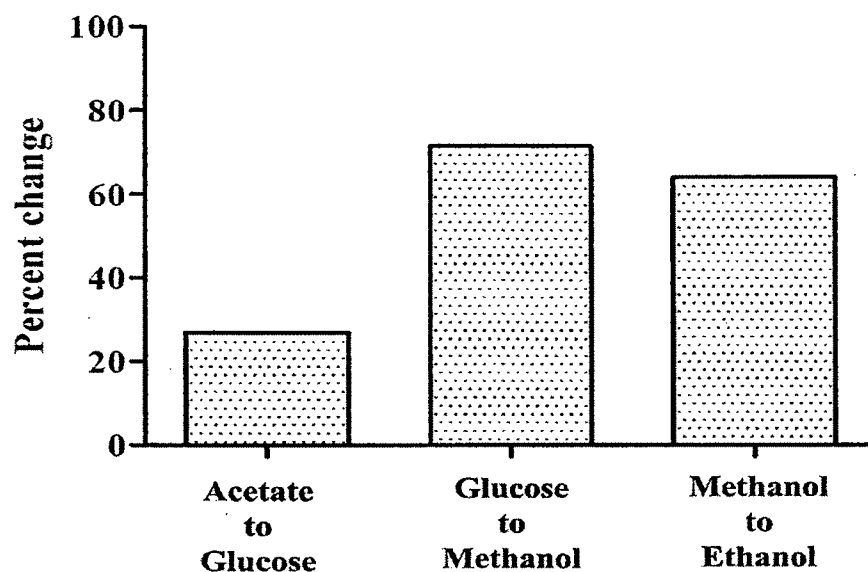


Fig. 4.8. Moving window analysis showing the percent change of the biofilm community with transition of carbon source

Table 4.2. Diversity indices calculated from the DGGE band patterns

| Carbon source | Simpson's index (D^{-1}) | reciprocal Shannon-Weiner index (H) | Evenness (E) |
|---------------|------------------------------|-------------------------------------|--------------|
| Acetate | 6.379 | 2.052 | 0.825 |
| Glucose | 9.048 | 2.364 | 0.872 |
| Methanol | 9.113 | 2.371 | 0.953 |
| Ethanol | 7.864 | 2.178 | 0.803 |

Table 4.3. 16S rRNA gene similarity to the closely related organism from the eluted bands of DGGE

| Band | Sequence length (bases) | Most closely related organism | Percent similarity |
|------|----------------------------|--|-----------------------|
| A | 130 | <i>Methylobacillus</i> sp. (GU937478.1) | 95 |
| B | 140 | <i>Enterobacter</i> sp. (GQ383912.1) | 96 |
| C | 132 | Uncultured <i>Chryseobacterium</i> clone (EF033490) | |
| D | 134 | <i>Alcaligenes faecalis</i> (FJ984837.1) | 98 |
| E | 138 | <i>Pseudomonas stutzeri</i> (CP002622) | 100 |
| F | 85 | <i>Pseudomonas</i> sp. (HM920246.1) | 95 |
| G | 138 | <i>Alcaligenes faecalis</i> (JF297973) | 96 |
| H | 137 | <i>Pseudomonas</i> sp. (HM920246.1) | 95 |
| I | 127 | Uncultured bacterium clone (FJ798920.1) | 95 |
| J | 149 | <i>Enterobacter</i> sp. (AY744934.1) | 99 |
| K | 98 | Uncultured bacterium clone (GU003710) | 94 |

* Parenthesis contain the accession numbers

4.3.5. *Pseudomonas* sp. dominates the biofilm by colonizing the surface initially

Although community change was observed in the biofilm with different carbon sources, *Pseudomonas* sp. were found to be numerically dominant in all of them including the *Alcaligenes* sp. present in considerable density. We hypothesized that the initial colonization of the substratum surface by the *Pseudomonas* sp. possibly conferred them the benefit to stay dominant even with fluctuations in the carbon source. Hence, we probed the biofilm development by analysing the spatial distribution of *Pseudomonas* sp., *Alcaligenes* sp. and *Paracoccus* sp. through FISH and confocal microscopy. It was observed that the *Pseudomonas* sp. dominated the biofilm throughout the development and *Paracoccus* sp. showed the lowest amount of intensity up to 24 days (Fig. 4.9 A-E). However the ratio of

fluorescent intensity between *Alcaligenes* sp. to *Pseudomonas* sp. was in the range 0.12 to 0.17 except 0.35 at the 18th day (Fig. 4.10). The *Paracoccus* to *Pseudomonas* sp. intensity ratio was in the range 0.01 to 0.17 with 0.37 at the 30th day (Fig. 4.10). The sum of intensities in the Z-stack of each probe was used to normalize the intensity value of each stack and these values of different fields were aggregated according to their percentage position from bottom (substratum surface) to the surface (towards bulk fluid phase) of the biofilm (Fig. 4.9 a-e). From this, a pattern was observed where the *Pseudomonas* sp. is in high numbers towards the base of the biofilm except the 18th day, which suggests that the *Pseudomonas* sp. colonizes the substratum surface from the initial period and the area covered is also more by the *Pseudomonas* sp. as viewed in the images (Fig. 4.9 a-e). Different species of *Pseudomonas* are known to lead the biofilm lifestyle in varied environments suggesting that the growth on surfaces as their prominent ecological niche (Moller et al. 1996; Auerbach et al. 2000; Parsek & Singh 2003; Danhorn & Fuqua 2007). Xavier and Foster (2007) proposed that the EPS production gives a selective advantage for organisms in a biofilm. Also, increased production of EPS by an overexpressing mutant is shown to increase biofilm formation in *Pseudomonas fluorescens* (Bianciotto et al. 2001). Production of copious amounts of EPS by different *Pseudomonas* species is reported (Roberson & Firestone 1992; Martin et al. 1993; Allison et al. 1998; Priester et al. 2006). *Pseudomonas* sp. also has a wide metabolic capability (Stanier et al. 1966). Thus the biofilm formation by production of EPS with a wide metabolic capacity has possibly made the organism colonize and thrive on surfaces.

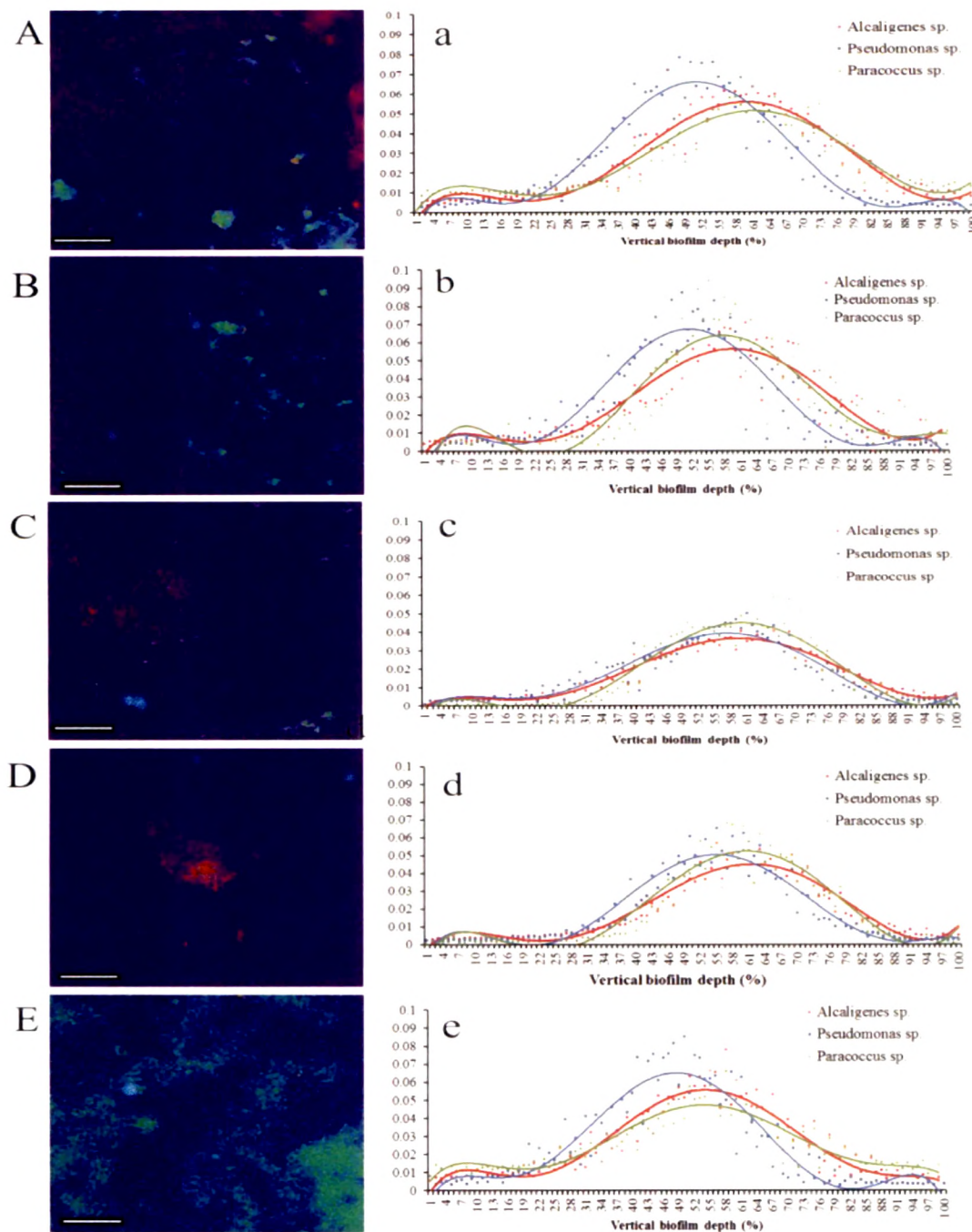


Fig. 4.9. FISH images acquired at 20X magnification during the biofilm development with corresponding graph showing the vertical distributions of the three species. y-axis in the graph denotes the normalization of the intensity values with the sum of the intensities in the z-stack. The 1 to 100% in the x-axis denotes the biofilm from the substratum surface towards the bulk fluid phase. Blue = *Pseudomonas* sp., red = *Alcaligenes* sp., green = *Paracoccus* sp. **A and a** - 6 days **B and b** - 12 days **C and c** - 18 days **D and d** - 24 days **E and e** - 30 days. Scale bar = 80 μ m

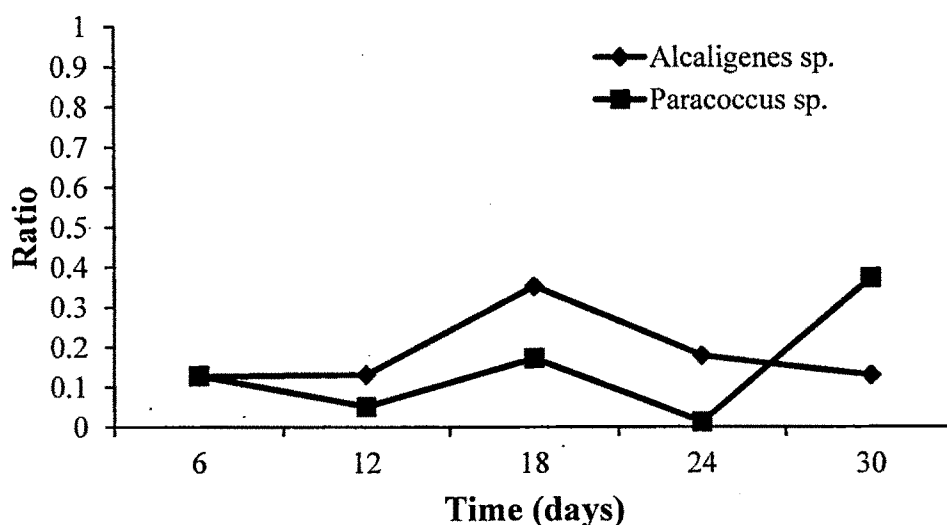


Fig. 4.10. The ratio of *Alcaligenes* sp. and *Paracoccus* sp. to *Pseudomonas* sp. during the biofilm development as analysed by the FISH image intensities

4.3.6. Increasing nitrate concentrations increase *Paracoccus* sp. in the community biofilm

Paracoccus species are generally found in denitrifying reactor sludge and also in biofilms (Neef et al. 1996). *Paracoccus* sp. W1b showed efficient denitrification in this study and there are also other reports showing efficient denitrification by different *Paracoccus* species. However, the bands sequenced from the DGGE gel (Table 4.3) did not show similarity to *Paracoccus* sp. But the FISH results showed *Paracoccus* sp. to stay in low density in the biofilm formed when acetate was used as the carbon source. Previous experiments in the chapter 2 showed the *Paracoccus* sp. isolate could tolerate and denitrify high nitrate concentrations. Hence, the biofilm community formed in the reactor in presence of acetate as the sole carbon source was inoculated with the *Paracoccus* sp. W1b culture and, quantified by FISH and compared with the already dominant *Pseudomonas* sp.

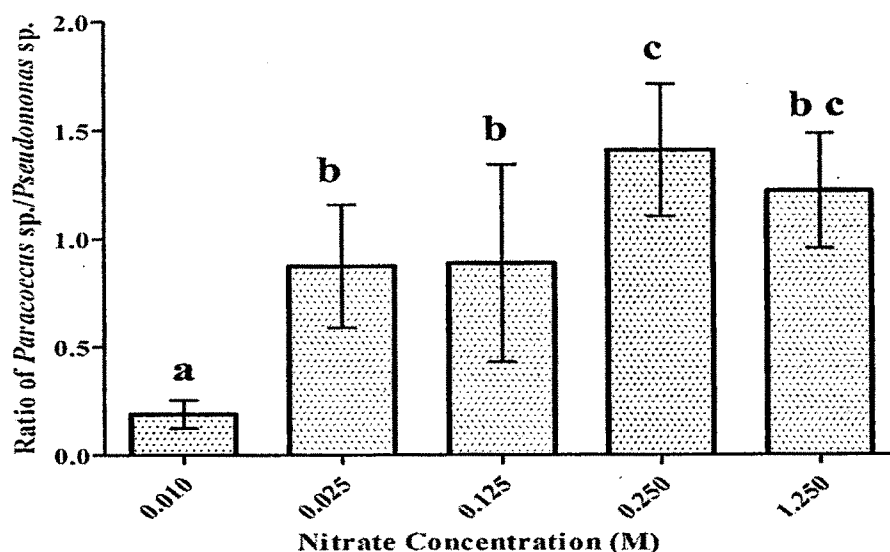


Fig. 4.11. Ratio of the *Paracoccus* sp. to *Pseudomonas* sp. intensity values in the biofilm. Error bars represent standard deviation. One way ANOVA with Tukey's test was used to determine significant differences. Different letters above the bars indicate significant difference $p < 0.05$

It was observed that with the increasing nitrate concentration in the influent, the ratio of *Paracoccus* sp. increased as compared to the *Pseudomonas* sp. The *Pseudomonas* sp. was found to dominate the biofilm in presence of the four different carbon sources used and was also higher in acetate biofilm relatively (Fig. 4.7c). However, although the ratio of *Paracoccus* sp. was higher at increasing nitrate concentrations (Fig. 4.11), the substratum surface was colonized by *Pseudomonas* sp. (Fig. 4.12)

Nitric oxide, which is an intermediate in denitrification, is implicated in the dispersal of *Pseudomonas aeruginosa*. Denitrification of high nitrate concentrations increases the transient nitric oxide production and this can be the possible reason for the decrease of *Pseudomonas* sp. in the biofilm. Nevertheless, *Paracoccus* sp. showed tolerance to high nitrate concentrations and the intermediates of denitrification like the nitrite or nitric oxide did not affect the biofilm. This possibly increased the fitness of *Paracoccus* sp. to increase in the biofilm as had been hypothesized in chapter 2.

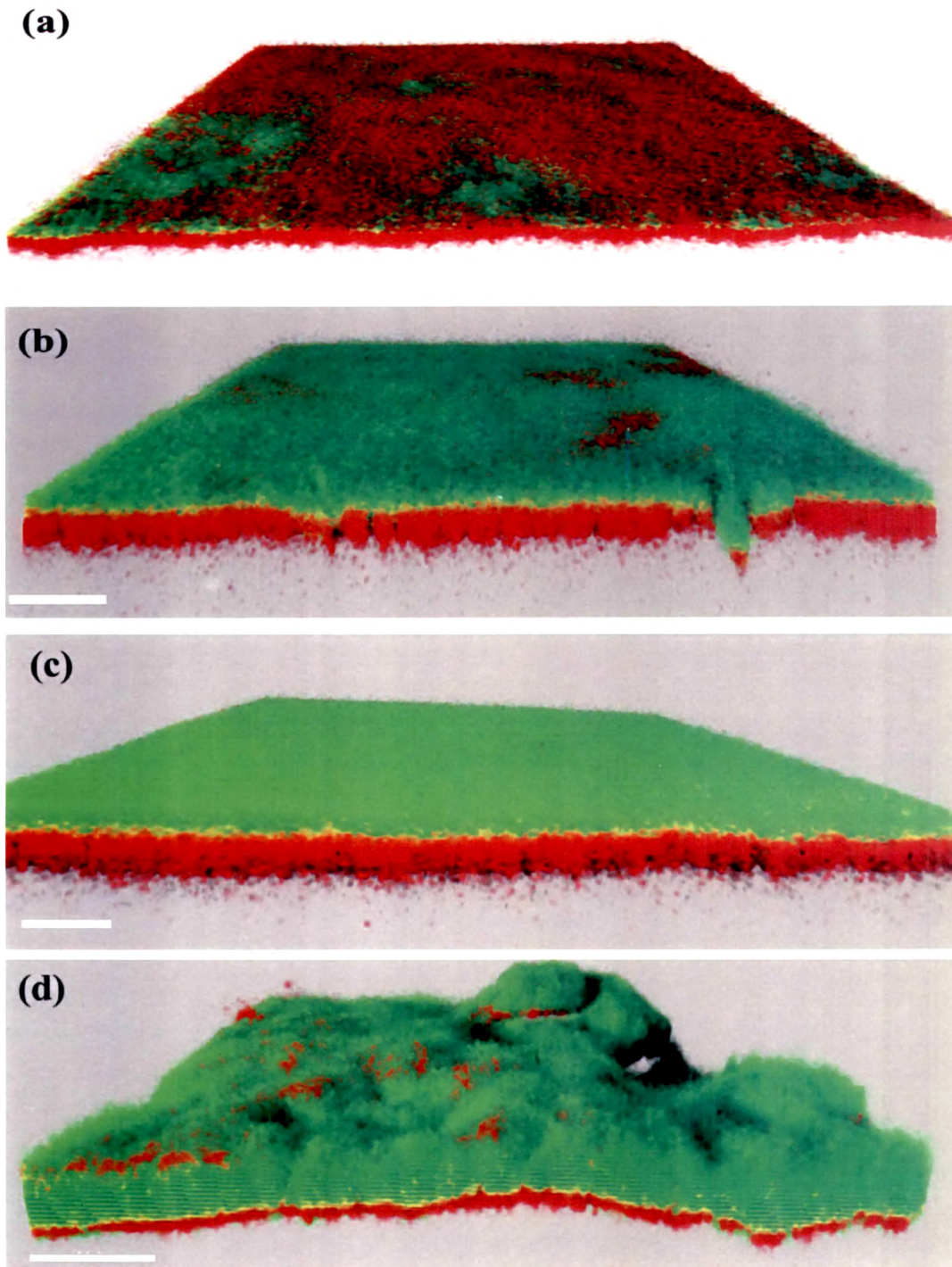


Fig. 4.12. Three dimensional images of the FISH involving the probes for the *Paracoccus* sp. (green) and *Pseudomonas* sp. (red) of the community biofilm grown in the synthetic wastewater containing different nitrate concentrations of (a) 10 mM (b) 25 mM (c) 125 mM (d) 250 mM (e) 1.25 M

From this study it was seen that the biofilm, when provided with acetate as a sole carbon source is efficient in nitrate removal by denitrification without accumulation of the intermediates (Fig. 1). The efficiency of denitrification conferred by acetate is possibly because of the many factors including increase in denitrifying community as compared to the nitrate ammonifiers in the biofilm (Fig. 5 & Table 3) and forming a denitrification-supportive biofilm structure with high thickness, diffusion distance and more biomass (Fig. 4). Glucose-fed biofilm reduce nitrate efficiently but with accumulation of nitrite and ammonium (Fig. 1) by helping the growth of nitrate ammonifying bacteria in high numbers (Fig. 5) which compete with denitrifiers in reducing nitrate, which is not desired in the reactors. Though species richness was high in methanol-fed biofilm (Table 2), the denitrification was not very efficient with increased accumulation of nitrite (Fig. 1). Ethanol as a carbon source supports denitrifying bacteria in high numbers (Table 1) but the denitrification was not efficient probably because of the non-supportive biofilm structure with relatively low thickness and diffusion distance (Fig. 4). However if the specific denitrifying activity is calculated by the biomass data of the biofilm, then the ethanol biofilm shows the highest specific activity. The succession of bacteria also occurs in a predictive fashion as supported by the literature where the Enterobacteriaceae family dominates when glucose is provided as the carbon source and *Methylobacillus* sp. dominates in methanol, while *Pseudomonas* sp. stays in high numbers because of their initial surface colonization and wide metabolic capability. *Paracoccus* sp. population increases at high nitrate concentration in the biofilm, though *Pseudomonas* sp. was shown to colonize the surfaces.

4.4. References

- Akunna, J. C., Bizeau, C., Moletta, R., (1993), Nitrate and nitrite reductions with anaerobic sludge using various carbon sources: glucose, glycerol, acetic acid, lactic acid and methanol. *Water Res.* 27, 1303-1312.
- Allison, D.G., Ruiz, B., SanJose, C., Jaspe, A., Gilbert, P., (1998), Extracellular products as mediators of the formation and detachment of *Pseudomonas fluorescens* biofilms. *FEMS Microbiol Lett.* 167, 179-184.
- Auerbach, I. D., Sorensen, C., Hansma, H. G., Holden, P. A., (2000), Physical morphology and surface properties of unsaturated *Pseudomonas putida* biofilms. *J Bacteriol.* 182, 3809-3815.
- Bent, S. J., Pierson, J.D., Forney, L. J., (2007), Measuring species richness based on microbial community fingerprints: the emperor has no clothes. *App Env Microbiol.* 73, 2399-2401.
- Bianciotto, V., Andreotti, S., Balestrini, R., Bonfante, P., Perotto, S., (2001), Mucoid mutants of the biocontrol strain *Pseudomonas fluorescens* CHA0 show increased ability in biofilm formation on mycorrhizal and nonmycorrhizal carrot roots. *MPMI.* 14, 255-260.
- Constantin, H., Fick, M., (1997), Influence of C-sources on the denitrification rate of a high nitrate concentrated industrial wastewater. *Water Res.* 31, 583-589.
- Daims, H., Stoecker, K., Wagner, M., (2005), *Fluorescence In Situ Hybridization* for the detection of prokaryotes. In Mark Osborn and Cindy Smith (eds). *Molecular Microbial Ecology*. Taylor & Francis, New York, NY 213-239.
- Danhorn, T., Fuqua, C., (2007), Biofilm formation by plant-associated bacteria. *Annu Rev Microbiol.* 61, 401-422.
- deBeer, D., Stoodley, P., Roe, F., Lewandowski, Z., (1994), Effects of biofilm structures on oxygen distribution and mass transport. *Biotech Bioeng* 43, 1131-1138.
- Dincer, A. R., Kargi, F., (2000), Kinetics of sequential nitrification and denitrification processes. *Enz Microb Tech.* 27, 37-42.
- Elefsiniotis, P., Wareham, D .G., (2007), Utilization patterns of volatile fatty acids in the denitrification reaction. *Enz Microb Tech.* 41, 92-97.
- Ginige, M. P., Keller, Jr., Blackall, L. L., (2005), Investigation of an acetate-fed denitrifying microbial community by stable isotope probing, full-cycle rRNA

- analysis, and fluorescent in situ hybridization-microautoradiography. *App Env Microbiol.* 71, 8683–8691.
- Gomez, M. A., Galvez, J. M., Hontoria, E., Gonzalez-Lopez, J., (2003), Influence of ethanol concentration on biofilm bacterial composition from a denitrifying submerged filter used for contaminated groundwater. *J Biosc Bioeng.* 95, 245-251.
- Hallin, S., Rothman, M., Pell, M., (1996), Adaptation of denitrifying bacteria to acetate and methanol in activated sludge. *Water Res.* 30, 1445-1450.
- Henry, S., Bru, D., Stres, B., Hallet, S., Philippot, L., (2006), Quantitative detection of the *nosZ* gene, encoding nitrous oxide reductase, and comparison of the abundances of 16S rRNA, *narG*, *nirK*, and *nosZ* genes in soils. *App Env Microbiol.* 72, 5181–5189.
- Her, J-J., Huang, J-S., (1995), Influences of carbon source and C/N ratio on nitrate/nitrite denitrification and carbon breakthrough. *Biores Tech.* 54, 45-51.
- Heydorn, A., Nielsen, A. T., Hentzer, M., Sternberg, C., Givskov, M., Ersboll, B. K., Molin, S., (2000), Quantification of biofilm structures by the novel computer program COMSTAT. *Microbiology.* 146, 2395-2407.
- Kim, S. W., Kim, B. H., Kim, Y. M., (1991), A *Methylobacillus* isolate growing only on methanol. *Kor J Microbiol.* 29, 250-257.
- Labbe, N., Laurin, V., Juteau, P., Parent, S., Villemur, R., (2007), Microbiological community structure of the biofilm of a methanol-fed, marine denitrification system, and identification of the methanol-utilizing microorganisms. *Microb Eco.* 53, 621–630.
- Lee, N. M., Welander, T., (1996), The effect of different carbon sources on respiratory denitrification in biological wastewater treatment. *J Ferm Bioeng.* 82, 277-285.
- Martin, D. W., Schurr, M. J., Mudd, M. H., Govan, J. R.W., Holloway, B. W., Deretic, V., (1993), Mechanism of conversion to mucoidy in *Pseudomonas aeruginosa* infecting cystic fibrosis patients. *Proc Nat Acad Sci.* 90, 8377-8381.
- Mateju, V., Cizinska, S., Krejci, J., Janoch, T., (1992), Biological water denitrification - A review. *Enz Microb Tech.* 14, 170-183.
- Moller, S., Pedersen, A. R., Poulsen, L. K., Arvin, E., Molin, S., (1996), Activity and three-dimensional distribution of toluene-degrading *Pseudomonas putida* in a

- multispecies biofilm assessed by quantitative In Situ hybridization and scanning confocal laser microscopy. *Appl Env Microbiol.* 62, 4632-4640.
- Neef, A., Zeglauer, A., Meier, H., Amann, R., Lemeer, H., Schleifer, K-H., (1996), Population analysis in a denitrifying sand filter: conventional and in situ Identification of *Paracoccus* spp. in methanol-fed biofilms. *Appl Env Microbiol.* 62, 4329-4339.
- Park, J. Y., Yoo, Y. J., (2009), Biological nitrate removal in industrial wastewater treatment: which electron donor we can choose. *Appl Microbiol Biotech.* 82, 415-429.
- Parsek, M. R., Singh, P.K., (2003,) Bacterial Biofilms: An Emerging Link to Disease Pathogenesis. *Annu Rev Microbiol.* 57, 677-701.
- Philippot, L., Hallin, S., (2005), Finding the missing link between diversity and activity using denitrifying bacteria as a model functional community. *Curr Opin Microbiol.* 8, 234-239.
- Priester, J. H., Olson, S. G., Webb, S. M., Neu, M. P., Hersman, L. E., Holden, P.A., (2006), Enhanced exopolymer production and chromium stabilization in *Pseudomonas putida* unsaturated Biofilms. *App Env Microbiol.* 72, 1988-1996.
- Roberson, E. B., Firestone, M. K., (1992), Relationship between desiccation and exopolysaccharide production in a soil *Pseudomonas* sp. *App Env Microbiol.* 58, 1284-1291.
- Rutting, T., Boeckx, P., Muller, C., Klemetsson, L., (2011), Assessment of the importance of dissimilatory nitrate reduction to ammonium for the terrestrial nitrogen cycle. *Biogeosc Disc.* 8, 1169-1196.
- Stanier, R. Y., Palleroni, N. J., Doudoroff, M., (1966), The aerobic Pseudomonads: a taxonomic study. *J Gen Microbiol.* 43, 159-271.
- Strohm, T. O., Griffin, B., Zumft, W. G., Schink, B., (2007) Growth yields in bacterial denitrification and nitrate ammonification. *Appl Env Microbiol.* 73, 420-424.
- Tiedje, J. M., Sextone, A. J., Myrold, D. D., Robinson, J. A., (1982), Denitrification: ecological niches, competition and survival. *Antonie van Leeuwenhoek.* 48:569-583.
- Urakami, T., Komagata, K., (1986), Emendation of *Methylobacillus* Yordy and Weaver 1977, a genus for methanol-utilizing bacteria. *Int J syst Bacteriol.* 36, 502-511.

- Watt, M., Hugenholtz, P., White, R., Vinall, K., (2006), Numbers and locations of native bacteria on field-grown wheat roots quantified by fluorescence in situ hybridization (FISH). *Env Microbiol.* 8, 871-884.
- Wellinghausen, N., Wirths, B., Poppert, S., (2006) *Fluorescence In Situ Hybridization* for rapid identification of *Achromobacter xylooxidans* and *Alcaligenes faecalis* recovered from cystic fibrosis patients. *J Clin microbial.* 44, 3415-3417.
- Wittebolle, L., Boon, N., Vanparys, B., Heylen, K., Vos, P. D., Verstraete, W., (2005), Failure of the ammonia oxidation process in two pharmaceutical wastewater treatment plants is linked to shifts in the bacterial communities. *J App Microbiol.* 99, 997–1006.
- Xavier, J. B., Foster, K.R., (2007), Cooperation and conflict in microbial biofilms. *Proc Nat Acad Sci.* 104, 876–881.
- Zumft, W. G., (1997), Cell biology and molecular basis of denitrification. *Microbiol Mol Biol Rev* 61, 533–616.